Application of Ultrasonic Measurements for the Evaluation of Steel Fiber Reinforced Concrete

Belayhun Gebretsadik
Clark County Building and Fire Prevention
Las Vegas, USA
belayhun.gebretsadik@ClarkCountyNV.gov

Kazem Jadidi
Department of Civil and Environmental Engineering and Construction, University of Nevada, Las Vegas, USA
kazem.jadidi@unlv.edu

Visar Farhangi
Department of Civil and Environmental Engineering and Construction, University of Nevada, Las Vegas, USA
farhangi@unlv.nevada.edu

Moses Karakouzian
Department of Civil and Environmental Engineering and Construction, University of Nevada, Las Vegas, USA
mkar@unlv.nevada.edu

Abstract-This study investigates the feasibility of the application of ultrasonic measurement to characterize Steel-Fiber-Reinforced Concrete (SFRC). Specifically, the effects of steel fiber content, age, moisture content, and fiber orientation on Ultrasonic-Pulse-Velocity (UPV) were investigated. In this regard, beam and cylindrical samples were fabricated with different steel fiber contents. The result indicated that for beam specimens the UPV increases with the addition of fiber up to 2% and decreases for higher fiber percentages. Additionally, the fiber orientation within the beam specimens influences the UPV measurements. For cylindrical samples, the rate of UPV decreased with the addition of steel fiber reinforcement. In addition, it was discovered that the curing period affects the magnitude of UPV.

Keywords-NDT; ultrasound; concrete; steel fiber; curing; pulse velocity; orientation

I. INTRODUCTION

Concrete is used extensively in most construction projects because its constituent materials are locally available. It has high compressive strength, and it the lowest cost-to-strength ratio compared to other available materials [1-5]. Some of the characteristics of plain concrete are its low tensile strength and its low tensile strain capacities. Concrete is a brittle material [6-10]. Therefore, improving the ductility of concrete is very important, especially due to the fact that concrete structures may experience extreme loadings during their lifetime [11-14]. To address such a deficiency, a continuous reinforcing bar has been applied to resist the tensile force imposed on the structure [15-18]. Unlike continuous reinforcing bars, fibers are short, discontinuous, and randomly distributed throughout the concrete to produce a more ductile and crack control matrix. Fibers used in concrete [18-21] can be made of steel, glass, and polymer. Authors in [22-23] investigated the mechanical behavior of polymers by infusing machine learning algorithms and asserted the advantages of using polymers on concrete's characteristics which is applicable to real-world problems [12, 18]. The random and closely spaced distribution of steel fibers enabled them to control the development of cracks better than continuous bars. It is important to recognize that, in general, fiber reinforcement is not a substitute for conventional reinforcement [24]. The addition of steel fibers in concrete can improve its toughness [14, 25-38], ductility, and post-crack resistance [29].

Self-Compacted Concrete (SCC) [30] is the concrete which is allowed to compact with its own weight without applying any vibrational effort. The reason for selecting SCC is to avoid steel fiber and aggregate segregation and bleeding. The use of SCC has been gradually increasing [31]. Basically, steel fiber reinforced SCC is produced by introducing superplasticizers to improve the workability of the mix while reducing the water-binder ratio. Other supplementary cementitious materials are fly ash (FA) and silica fume [32-35]. Silica fume also plays an important role in the chemical reaction (hydration) process to improve strength [36]. Ultrasonic Pulse Velocity (UPV) is one of the most Dominant Nondestructive Test (NDT) methods of concrete characterization [37]. The most common application of ultrasonic surveying to evaluate materials is the monitoring of the wave travel time, both in direct and indirect transmission [38]. The basic idea the pulse velocity established is that the velocity of the pulse of compressional waves through a medium depends on the elastic properties and density of the medium [39]. Even though the application of ultrasonic pulse velocity for construction materials characterization was initiated three decades ago, its response through steel fiber reinforced SCC has not been identified yet. The main objective of this study is to investigate the response of ultrasonic pulse velocity through steel fiber reinforced SCC with respect to the volume fraction of steel fibers, curing periods (7, 28, and 90 days), steel fiber and aggregate orientations, and wet/dry conditions.

II. METHODOLOGY

The direct-contact through transmission UPV test method was employed in this experiment. Based on ASTM C597-09 "Standard Test Method for Pulse Velocity through Concrete," this method is based on wave generated by an electro-

Corresponding author: Visar Farhangi

mechanical transducer placed on the surface of the test specimen. This experiment follows the through-transmission method. Unlike the pulse-echo method, which relies on the reflected waves, the through-transmission method uses a separate transducer as a receiver. This test method can be applied to assess the uniformity and relative quality of concrete [40] in order to indicate the presence of voids and cracks. It also can be used to estimate the progress of cracks [41] and other deterioration kinds in the long run, by doing repeated tests on the same spot. Ultrasound measurements could be used for failure monitoring in reinforced concrete [42]. The test begins when an ultrasonic pulse is generated and transmitted for an electro-acoustic transducer, placed in contact with the surface of the concrete. After passing through the concrete, the vibrations are received and converted by the electro-acoustic transducer placed on the opposite face. The travel time (μs) and energy loss (dB) are displayed on the digital screen. A coupling agent, such as gel, should be applied between the transducers face and specimen's surface to ensure that there is no air pocket between them. It is also equally important to align the two transducers so that the measured distance and the actual path length for the wave have a perfect match.

III. EXPERIMENTAL PROCEDURE AND MATERIALS

In this study, the main variables are steel fiber content, sample saturation, curing periods, fiber orientation, and porosity. The effects of fiber content, ranging from 0-4% (by volume), on ultrasonic pulse velocity were investigated. In addition, the variation of UPV through the saturated and air dried samples was also assessed. The curing periods were 7, 28, and 90 days. The steel fiber orientation effects were also studied. ASTM A 820-90 Type II deformed cut sheet carbon steel fibers were used, having an equivalent diameter of 0.584mm and a length of 19.05mm. The specific gravity of carbon steel fiber was 7.85g/cm^3, which is much higher than any of the constituent materials. The steel fibers had rectangular cross-sections with dimensions of 0.406×0.838×19.05mm. The tensile strength of the steel fibers ranged between 379 to 763MPa. These fibers were selected in order to get a strong bondage between the concrete matrix and steel fibers which in turn would improve the ductility of concrete. Coarse and fine aggregates were obtained from a local quarry in Las Vegas, Nevada area. Since the intended objective of this concrete mix design was ultimately to be used for thin plates and shells (about 25.4mm thick), the size of the coarse aggregates was limited to nominal sizes of 9.53mm and a #4 sieve. The type of aggregate used was crushed limestone. To meet the required gradation, pure natural sand fine aggregates were added to the mix. ASTM C 150 Type V Ordinary Portland Cement (OPC), 404kg/m^3, was used to prepare the test specimens. Type V OPC has a high sulfate resistance and lower setting time than Type I OPC. Table I presents the sieve analysis of the fine aggregates used in this study. The fineness modulus of the fine aggregates was 3.04. Both the gradation and the fineness modulus meet the ASTM C33 standards. The oven-dry specific gravity and absorption percentages of the fine aggregates following the ASTM C 128-07-a were 2.78 and 0.65 respectively.

TABLE I. FINE AGGREGATE SIEVE ANALYSIS

Sieve number	Passing percentage	Fine aggregates	
		Min(%)	Max(%)
4	100	95	100
8	90	80	100
16	55	50	85
30	30	25	60
50	15	5	30
100	6	0	10

Class F FA, 171kg/m^3 was used in this experiment. For this type of FA, the Blaine fineness and specific gravities are 5.23×103cm^2/g and 2100kg/m^3 respectively. FA is an important admixture to improve the workability and reduce the demand of cement or fine fillers in Steel Fiber Reinforced SCC (SFR-SCC). It has a great role in creating a sufficient amount of cement paste in SFR-SCC and improves the mechanical properties by filling the micro-pores in it [43]. Silica fume consists of small-sized particles approximately 100 to 150 times smaller than Portland cement particles, and has a high surface area and high amount of silicon dioxide. Silica fume with unit weight of 30.4kg/m^3 was used in this experiment. This silica fume was selected for its chemical and physical benefits. Superplasticizers, also known as High Range Water Reducers (HRWR), play an important role to improve concrete workability and strength in SFR-SCC with FA and silica fume [44]. ADVA 140 HRWR was selected for this experiment as superplasticizer. A constant amount of 6.3kg/m^3 HRWR was added to the cylindrical samples of the variable fiber content. The HRWR content varies with steel fiber content for the beam samples.

A. Mix Proportions

The mix proportion was designed so as to improve the common drawback (i.e. brittleness) of concrete and other mechanical properties. It consists of coarse aggregates, fine aggregates (sand), cement, FA, silica fume, water, superplasticizer, and deformed steel fibers as shown in Tables I and II. Except for the volume percentage (V_f) of steel fibers and superplasticizers, all the other constituent materials were kept constant for the beam samples. The amounts of superplasticizers were selected to provide the best workable concrete matrix for the respective percentages of steel fibers by trials and errors. The cylindrical samples, on the other hand, have all the constituent materials constant except the percentage volume steel fibers. However, unlike the beam samples, the amount of superplasticizer was kept constant for the cylindrical samples at 6.3kg/m^3 which was best for 0% fiber concrete workability, and adapted for the rest just for the sake of minimizing the number of variables and to realize the sole effect of steel fiber volumes in SFRC. Slump spread (ASTM C 1611), J-Ring flow (ASTM C 1621), V-Funnel and U-Box (ASTM C09.47) tests were conducted on non-reinforced fresh concrete. The results showed an average slump spread diameter of 759mm, flow diameter of 768.4mm with regard to J-Ring test, and 8s flow time based on V-Funnel test and 1.52mm for U-Box test respectively.

B. Specimen Preparation

A total of 18 beam and 5 cylindrical samples were prepared for this experiment. The main experimental program is based

on the beam samples since relatively representative samples were already available. However, since the beam samples were aged (more than a year), it was not possible to see the curing period effect. Therefore, cylindrical samples were prepared to investigate the curing period effect on UPV. Various studies suggest different fiber contents ranging from 1.5% to 6% [45], in order to reinforce the concrete specimens. In this study, the 18 beam samples were categorized in 5 groups: four of them had 4 members with steel fibers volumes of 0%, 1%, 2%, and 3%, respectively, and the fifth had 2 members with 4% fiber volume. Similarly, the cylindrical samples had 3 groups: 1 (0%), 2 (1%), and 3 (2%) of steel fibers percentage respectively. The dimensions of all beam and cylindrical samples were 10cm×10cm×35cm and 10cm ϕ×20cm respectively. Except for the amount of superplasticizers at 1% and 2% fibers, all the constituent materials were the same for all the cylindrical and beam samples. Dry mixing of coarse aggregates, fine aggregates, cement, FA, silica fume, and steel fibers were performed for about 1-2min with a mechanical mixer. Then, about 80% of the water was added and mixed thoroughly for the specified time. Finally, the remaining portion of water and HRWR were added at the end before discharging the mix. The concrete matrix was poured into the mold and allowed to set without any vibration effort (i.e. SCC). The samples were prepared based on ASTM C 192. Figure 1 presents the prepared beam and cylindrical samples.

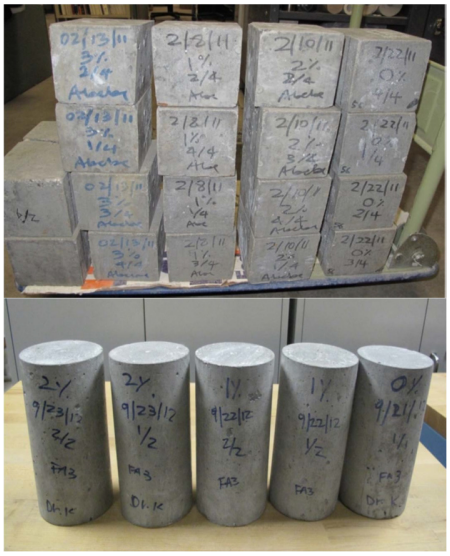

Fig. 1. Prepared beam and cylindrical samples.

C. Test Procedure

Once the instrument was set up, the next critical step was testing. This was critical because most errors occur in this part of the experiment. Before starting the experiment, the test specimen was placed on a level and stable surface. A digital caliper was used to measure the length of specimen along the direction of the wave. A gel was applied on both faces of the specimen where the transducers were to be placed so that the two faces of the transducers and test specimen had full contact. There should not be any uneven surface and/or air pockets between the transducers and specimen contact faces. Also, the two transducers needed to be aligned so that the measured dimensions and assumed wave travel path were the same. The same amount of pressure was applied on the two transducers to avoid the instability of amplitude of the wave, as shown in Figure 2. Moreover, 28-day compressive and flexural strength tests were performed on cylindrical specimens. The results are presented in Tables IV and V.

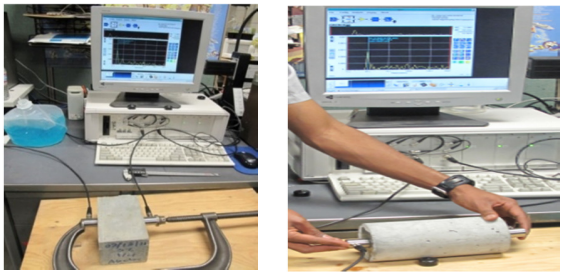

Fig. 2. UPV testing.

TABLE II. MIX PROPORTIONS FOR BEAM SAMPLES

Mix Category (percent fiber, by volume)					
Mix component	**0%**	**1%**	**2%**	**3%**	**4%**
3/8" coarse aggregate	22.8	22.8	22.8	22.8	22.8
#4 (4.75mm) coarse agg.	22.4	22.4	22.4	22.4	22.4
Fine aggregates (sand)	57.6	57.6	57.6	57.6	57.6
Water	10.22	10.22	10.22	10.22	10.22
Cement type V	25	25	25	25	25
Silica fume	1.9	1.9	1.9	1.9	1.9
FA (class F)	10.7	10.7	10.7	10.7	10.7
Water/cement	0.41	0.41	0.41	0.41	0.41
HRWR (Superplasticizer)	0.392	0.372	0.416	0.432	0.472
Steel fibers by volume	0	1	2	3	4
Steel fibers by weight	0	1.25	2.5	3.75	5

TABLE III. MIX PROPORTIONS FOR CYLINDRICAL SAMPLES

Mix category (percent fiber, by volume)			
Mix component	**0%**	**1%**	**2%**
3/8" coarse aggregate	22.8	22.8	22.8
#4 (4.75mm) coarse agg.	22.4	22.4	22.4
Fine aggregate (sand)	57.6	57.6	57.6
Water	10.22	10.22	10.22
Cement type V	25	25	25
Silica fume	1.9	1.9	1.9
FA (class F)	10.7	10.7	10.7
Water/cement	0.41	0.41	0.41
HRWR (Superplasticizer)	0.392	0.392	0.392
Steel fibers by volume	0	1	2
Steel fibers by weight	0	1.25	2.5

TABLE IV. COMPRESSIVE TEST RESULTS

Fiber content (%)	**0**	**1**	**2**	**3**	**4**
Compressive strength (MPa)	67.98	75.31	80.72	85.80	73.18

TABLE V. FLEXURAL STRENGTH RESULTS

Fiber content (%)	**0**	**1**	**2**	**3**	**4**
Load capacity (N)	30154	32529	35475	38662	37036

IV. RESULTS AND DISCUSSION

The objective of this study was to investigate the responses of UPV within steel fibers reinforced SCC. Interpreting the

results and drawing conclusions are more difficult and challenging tasks than in any conventional destructive test methods. Understanding the behaviors of ultrasonic wave velocity and its response to various factors within and around the test specimens are very important. The results are presented in the following paragraphs.

A. Cylindrical Specimen Results

For cylindrical specimens, the UPV measurement results are shown in Figure 3. Generally, adding certain amounts of steel fibers increases the UPV of the mix due to its high specific gravity. Hence, it was expected that the 0% fiber sample would have lower UPV rate in comparison to specimens with higher fiber percentages. However, for cylindrical samples the opposite was observed. We are not sure why this happened. Therefore, the highest UPV was observed for the samples with 0% fiber in comparison to samples with 1% and 2% fibers respectively. Moreover, the curing period had significant influence on the value of the UPV test result, specifically for unreinforced samples. The pulse velocity increased rapidly at an early period for the specimen with 0% steel fibers, while for fiber reinforced samples, the amount of UPV for 7 days and 28 days cured samples is not remarkable, due to the fact that for unreinforced specimens the main portion of the hydration process and gap filling were carried out within the early period of 28 days. On the other hand, the concrete got its maximum strength and density, during this period. While the presence of 1% and 2% steel fiber, delayed/retarded the gap filling or consolidation time of concrete, hence, the UPV increased gradually and over a longer period of time. This is a good indication of the UPV can be used to estimate the setting time of concrete. For both reinforced and unreinforced samples, the highest UPV was observed after 90 days of curing.

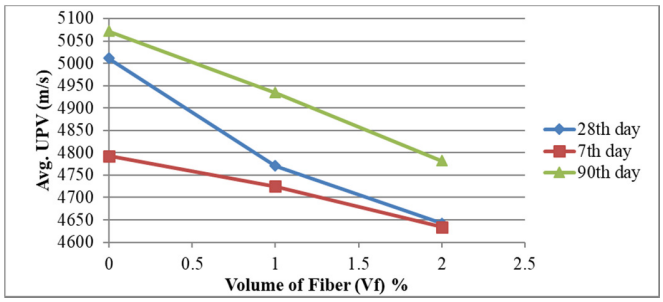

Fig. 3. Effect of the volume of steel fibers (V_f) % on UPV for cylindrical samples.

B. Beam Specimen Results

For beam specimens, UPV measurement was performed along three perpendicular sides of the specimen as shown in Figure 4. The results are shown in Figure 5. The presence of short, deformed, and randomly distributed steel fibers affected the UPV measurement both positively and negatively. For all beam sections, the addition of up to 2% steel fibers to a plain concrete increased the average pulse velocity. However, further addition of fibers did not improve either the UPV or other concrete properties. The reason could be that since the test samples were self-consolidated samples, the addition of more fibers initiated the formation of voids thus reducing the workability of the matrix. This, in-turn, decreased the speed of wave propagation through the sample and resulted in a lower UPV value. Though a properly match HRWR superplasticizer was added to the mix to improve its workability, the problem could not be solved and was even pronounced for higher fiber volume (4%). On the other hand, the lowest UPV was observed to 6% steel fiber specimens. Therefore, for a steel-fiber-reinforced, self-compacted concrete, 2% by volume of steel fiber may be the recommended optimum amount to be added to improve the properties of concrete structures with a corresponding superplasticizer.

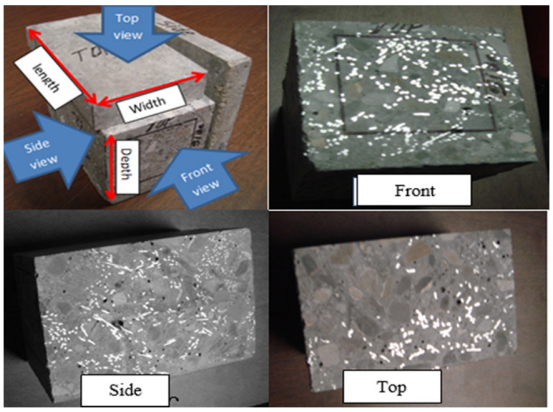

Fig. 4. Fiber orientations of a beam sample.

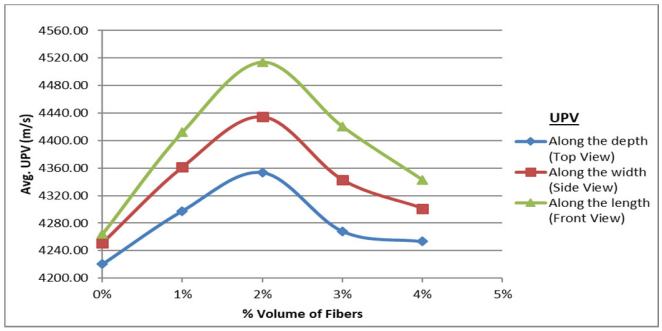

Fig. 5. Effects of fiber and aggregate orientation on UPV for beam specimens.

A remarkable difference was observed for UPV measurements taken from different planes of the beam specimens. Although all samples were self-consolidated, there seems to be a tendency for the aggregates and fibers to orient along the horizontal length and width of the specimen. The approximate count per square inch concentrations of fiber orientation can be estimated as 11.6fibers/in^2, 32fibers/in^2, and 50fibers/in^2 on the top plane, side plane, and front plane, respectively which corresponds to the UPV measurements. Accordingly, fiber orientation needs to be considered in evaluating the effect of the fibers on the strength of the fiber reinforced concrete. The orientation of steel fibers aligned with the horizontal plane is recommended for achieving the maximum concrete tensile strength, which would be comparable to the strength provided by vibrated FRC. For similar samples, the UPV was higher along the direction where the more fibers were oriented. The differences between the

UPV readings along the length and the depth were cumulative effects of both fibers and aggregate orientation, since they had different pivots at 0% fiber and the difference increased with the fibers' volume. Therefore, the fibers and aggregate orientation made a significant difference on the UPV value, which is increasing the UPV in the direction of fiber and aggregate orientation. The comparison in Table V and Figure 5 indicates an identical trend between beam load capacity and ultrasound test results although there are some differences. The beam load capacity increases with the increase in fiber content and then declines. The highest load capacity was observed for 3% fiber content while the ultrasound survey indicates the highest UPV for specimens reinforced with 2% fiber. The authors did not observe any trend between compressive strength and UPV results for the cylindrical specimens.

V. CONCLUSIONS

An ultrasonic survey was carried out on cylindrical and beam samples reinforced with various content percentages of steel fibers. The UPV was measured and analyzed. The results show as that:

- The optimum steel fiber content for beam sections is indicated to be 2%.
- With the addition of fiber reinforcement from 0% up to 2%, the amount of UPV increases for beam samples and then it decreases as fiber percentage increases from 2% to 6%.
- The fiber orientation needs to be considered in evaluating the effect of the fibers on the strength of the fiber reinforced concrete.
- The magnitude of UPV decreases for cylindrical samples with the addition of steel fibers.
- The curing period has inevitable influence on wave speed. For cylindrical samples the highest UPV is observed after 90 days of curing.

ACKNOWLEDGEMENT

The authors appreciate the contribution of Professor Saman Ladkany and Dr. Abebe Tadesse Berhe regarding the samples' data.

REFERENCES

[1] Y. Wu, J. C. Ashlock, B. Cetin, S. Satvati, C. Li, and H. Ceylan, "Mechanistic Performance Evaluation of Chemically and Mechanically Stabilized Granular Roadways," in *Geo-Congress 2020*, Feb. 2020, pp. 591–601, https://doi.org/10.1061/9780784482810.061.

[2] A. Morovatdar, R. Ashtiani, C. Licon, and C. Tirado, "Development of a Mechanistic Approach to Quantify Pavement Damage Using Axle Load Spectra from South Texas Overload Corridors," in *Geo-Structural Aspects of Pavements, Railways, and Airfields (GAP 2019)*, Colorado Springs, CO, USA, Dec. 2019.

[3] V. Farhangi and M. Karakouzian, "Design of Bridge Foundations Using Reinforced Micropiles," presented at the International Road Federation Global R2T Conference & Expo, Las Vegas, NV, USA, Nov. 2019.

[4] S. Satvati, A. Nahvi, B. Cetin, J. C. Ashlock, C. T. Jahren, and H. Ceylan, "Performance-based economic analysis to find the sustainable aggregate option for a granular roadway," *Transportation Geotechnics*, Jul. 2020, Art. no. 100410, https://doi.org/10.1016/j.trgeo.2020.100410.

[5] A. Malakooti *et al.*, "Design and Full-scale Implementation of the Largest Operational Electrically Conductive Concrete Heated Pavement System," *Construction and Building Materials*, vol. 255, Sep. 2020, Art. no. 119229, https://doi.org/10.1016/j.conbuildmat.2020.119229.

[6] G. M. Colyvas, Y. Malecot, Y. Sieffert, S. Aboudha, and C. Kanali, "Behavior of Reinforced Concrete Beams using Wire Rope as Internal Shear Reinforcement," *Engineering, Technology & Applied Science Research*, vol. 10, no. 4, pp. 5940–5946, Aug. 2020, https://doi.org/10.48084/etasr.3496.

[7] V. Farhangi and M. Karakouzian, "Effect of Fiber Reinforced Polymer Tubes Filled with Recycled Materials and Concrete on Structural Capacity of Pile Foundations," *Applied Sciences*, vol. 10, no. 5, Jan. 2020, Art. no. 1554, https://doi.org/10.3390/app10051554.

[8] M. F. Sadeghian, P. A. Haddad, M. S. Jahandari, D. H. Rasekh, and D. T. Ozbakkaloglu, "Effects of electrokinetic phenomena on the load-bearing capacity of different steel and concrete piles: A small-scale experimental study," *Canadian Geotechnical Journal*, Jul. 2020, https://doi.org/10.1139/cgj-2019-0650.

[9] A. Asgharzadeh, H. Jamshidi Aval, and S. Serajzadeh, "A Study on Flow Behavior of AA5086 Over a Wide Range of Temperatures," *Journal of Materials Engineering and Performance*, vol. 25, no. 3, pp. 1076–1084, Mar. 2016, https://doi.org/10.1007/s11665-016-1927-5.

[10] R. Kumar, A. Kumar, and M. K. Kesharwani, "Steel Fiber Reinforced Concrete," *International Journal for Research in Applied Science and Engineering Technology*, vol. 7, no. 5, pp. 2456–2458, May 2019, https://doi.org/10.22214/ijraset.2019.5407.

[11] N. L. Dehghani and A. Shafieezadeh, "Probabilistic Sustainability Assessment of Bridges Subjected to Multi-Occurrence Hazards," in *International Conference on Sustainable Infrastructure 2019*, Nov. 2019, pp. 555–565, https://doi.org/10.1061/9780784482650.059.

[12] N. L. Dehghani, M. Rahimi, A. Shafieezadeh, and J. E. Padgett, "Parameter Estimation of a Fractional Order Soil Constitutive Model Using KiK-Net Downhole Array Data: A Bayesian Updating Approach," pp. 346–356, Feb. 2020, https://doi.org/10.1061/9780784482810.037.

[13] A. Valikhani, A. J. Jahromi, I. M. Mantawy, and A. Azizinamini, "Experimental evaluation of concrete-to-UHPC bond strength with correlation to surface roughness for repair application," *Construction and Building Materials*, vol. 238, p. 117753, Mar. 2020, https://doi.org/10.1016/j.conbuildmat.2019.117753.

[14] A. A. Ramezanianpour *et al.*, "Effect of Supplementary Cementing Materials on Concrete Resistance Against Sulfuric Acid Attack," in *High Tech Concrete: Where Technology and Engineering Meet*, Cham, 2018, pp. 2290–2298, https://doi.org/10.1007/978-3-319-59471-2_261.

[15] J. Sabzi, M. R. Esfahani, T. Ozbakkaloglu, and B. Farahi, "Effect of concrete strength and longitudinal reinforcement arrangement on the performance of reinforced concrete beams strengthened using EBR and EBROG methods," *Engineering Structures*, vol. 205, Feb. 2020, Art. no. 110072, https://doi.org/10.1016/j.engstruct.2019.110072.

[16] H. Shabani Attar, M. Reza Esfahani, and A. Ramezani, "Experimental investigation of flexural and shear strengthening of RC beams using fiber-reinforced self-consolidating concrete jackets," *Structures*, vol. 27, pp. 46–53, Oct. 2020, https://doi.org/10.1016/j.istruc.2020.05.032.

[17] M. Beizaei, E. S. Hosseininia, and A. Morovatdar, "Investigating the Practical Conditions to Utilize Brick Stair Wall Method as a Supporting Structure in Urban Excavation," pp. 429–439, Feb. 2020, https://doi.org/10.1061/9780784482797.042.

[18] A. Prabhakaran *et al.*, "Polymer Injection and Liquefaction-Induced Foundation Settlement: A Shake Table Test Investigation," in *Geo-Congress 2020*, Feb. 2020, pp. 1–9, https://doi.org/10.1061/9780784482810.001.

[19] R. Aghayari and M. Moradi, "Improving the Punching Shear Strength of RC Slabs by FRP and Steel Sheets," *Journal of Rehabilitation in Civil Engineering*, vol. 4, no. 1, pp. 1–17, Feb. 2016, https://doi.org/10.22075/jrce.2016.487.

[20] P. Arabali, S. Mirghaderi, and M. Shekarchi, "Constitutive Model for High Performance Fiber Reinforced Concrete under Triaxial Compression," in *The 2011 World Congress on Advances in Structural Engineering and Mechanics (ASEM' 11PLUS)*, Seoul, S. Korea, Sep. 2011.

[21] M. Kazemi *et al.*, "In-situ strength estimation of polypropylene fibre reinforced recycled aggregate concrete using Schmidt rebound hammer and point load test," *Journal of Sustainable Cement-Based Materials*, vol. 9, no. 5, pp. 289–306, Sep. 2020, https://doi.org/10.1080/21650373.2020.1734983.

[22] A. Ghaderi, V. Morovati, and R. Dargazany, "A Bayesian Surrogate Constitutive Model to Estimate Failure Probability of Rubber-Like Materials," *arXiv:2010.13241 [cond-mat]*, Oct. 2020, Accessed: Dec. 25, 2020. [Online]. Available: http://arxiv.org/abs/2010.13241.

[23] A. Ghaderi, V. Morovati, and R. Dargazany, "A Physics-Informed Assembly of Feed-Forward Neural Network Engines to Predict Inelasticity in Cross-Linked Polymers," *Polymers*, vol. 12, no. 11, Nov. 2020, Art. no. 2628, https://doi.org/10.3390/polym12112628.

[24] H. Behbahani, B. Nematollahi, and M. Farasatpour, "Steel fiber reinforced concrete : a review," 2011, Accessed: Dec. 25, 2020. [Online]. Available: http://dl.lib.mrt.ac.lk/handle/123/9505.

[25] B. Farahi, M. R. Esfahani, and J. Sabzi, "Experimental Investigation on the Behavior of Reinforced Concrete Beams Retrofitted with NSM-SMA/FRP," *Amirkabir (Journal of Science and Technology)*, vol. 51, no. 4, pp. 685–698, Oct. 2019, https://doi.org/10.22060/ceej.2018.13927.5512.

[26] A. Malakooti, M. Maguire, and R. J. Thomas, "Evaluating Electrical Resistivity as a Performance based Test for Utah Bridge Deck Concrete," Utah State University, Rutgers University, University Transportation Centers Program, CAIT-UTC-NC35, Jan. 2018. Accessed: Dec. 25, 2020. [Online]. Available: https://trid.trb.org/View/1532167.

[27] R. Afsharhasani, M. Karakouzian, and V. Farhangi, "Effect of Competent Caliche Layers on Measuring the Capacity of Axially Loaded Drilled Shafts Using the Osterberg Test," *Applied Sciences*, vol. 10, no. 18, Jan. 2020, Art. no. 6169, https://doi.org/10.3390/app10186169.

[28] S. A. Nazari Tiji *et al.*, "Characterization of yield stress surface and strain-rate potential for tubular materials using multiaxial tube expansion test method," *International Journal of Plasticity*, vol. 133, Oct. 2020, Art. no. 102838, https://doi.org/10.1016/j.ijplas.2020.102838.

[29] S. Zamanian, J. Hur, and A. Shafieezadeh, "A high-fidelity computational investigation of buried concrete sewer pipes exposed to truckloads and corrosion deterioration," *Engineering Structures*, vol. 221, Oct. 2020, Art. no. 111043, https://doi.org/10.1016/j.engstruct.2020.111043.

[30] A. Sadrmomtazi, S. H. Gashti, and B. Tahmouresi, "Residual strength and microstructure of fiber reinforced self-compacting concrete exposed to high temperatures," *Construction and Building Materials*, vol. 230, Jan. 2020, Art. no. 116969, https://doi.org/10.1016/j.conbuildmat.2019.116969.

[31] Y. Xie, B. Liu, J. Yin, and S. Zhou, "Optimum mix parameters of high-strength self-compacting concrete with ultrapulverized fly ash," *Cement and Concrete Research*, vol. 32, no. 3, pp. 477–480, Mar. 2002, https://doi.org/10.1016/S0008-8846(01)00708-6.

[32] M. Jalal, N. Nassir, H. Jalal, and P. Arabali, "On the strength and pulse velocity of rubberized concrete containing silica fume and zeolite: Prediction using multivariable regression models," *Construction and Building Materials*, vol. 223, pp. 530–543, Oct. 2019, https://doi.org/10.1016/j.conbuildmat.2019.06.233.

[33] S. A. Chandio, B. A. Memon, M. Oad, F. A. Chandio, and M. U. Memon, "Effect of Fly Ash on the Compressive Strength of Green Concrete," *Engineering, Technology & Applied Science Research*, vol. 10, no. 3, pp. 5728–5731, Jun. 2020, https://doi.org/10.48084/etasr.3499.

[34] P. Ghadir and N. Ranjbar, "Clayey soil stabilization using geopolymer and Portland cement," *Construction and Building Materials*, vol. 188, pp. 361–371, Nov. 2018, https://doi.org/10.1016/j.conbuildmat.2018.07.207.

[35] M. Ameri, B. Kalantari, and S. Jahandari, "Laboratory Study of Determination of Optimum Amount of Water and Clay in Mortar Made with Lime and Fly Ash," in *International conference on research in sience and technology*, Kualalumpur, Malaysia, Apr. 2015.

[36] S. Muzenski, I. Flores-Vivian, B. Farahi, and K. Sobolev, "Towards Ultrahigh Performance Concrete Produced with Aluminum Oxide Nanofibers and Reduced Quantities of Silica Fume," *Nanomaterials*, vol. 10, no. 11, Nov. 2020, Art. no. 2291, https://doi.org/10.3390/nano10112291.

[37] K. Güçlüer, "Investigation of the effects of aggregate textural properties on compressive strength (CS) and ultrasonic pulse velocity (UPV) of concrete," *Journal of Building Engineering*, vol. 27, Jan. 2020, Art. no. 100949, https://doi.org/10.1016/j.jobe.2019.100949.

[38] D. Bui, S. A. Kodjo, P. Rivard, and B. Fournier, "Evaluation of Concrete Distributed Cracks by Ultrasonic Travel Time Shift Under an External Mechanical Perturbation: Study of Indirect and Semi-direct Transmission Configurations," *Journal of Nondestructive Evaluation*, vol. 32, no. 1, pp. 25–36, Mar. 2013, https://doi.org/10.1007/s10921-012-0155-7.

[39] V. Dubey and A. Noshadravan, "A probabilistic upscaling of microstructural randomness in modeling mesoscale elastic properties of concrete," *Computers & Structures*, vol. 237, Sep. 2020, Art. no. 106272, https://doi.org/10.1016/j.compstruc.2020.106272.

[40] M. A. Kewalramani and R. Gupta, "Concrete compressive strength prediction using ultrasonic pulse velocity through artificial neural networks," *Automation in Construction*, vol. 15, no. 3, pp. 374–379, May 2006, https://doi.org/10.1016/j.autcon.2005.07.003.

[41] D. G. Aggelis, T. Shiotani, S. Momoki, and A. Hirama, "Acoustic Emission and Ultrasound for Damage Characterization of Concrete Elements," *Materials Journal*, vol. 106, no. 6, pp. 509–514, Nov. 2009, https://doi.org/10.14359/51663333.

[42] M. Rucka and K. Wilde, "Experimental Study on Ultrasonic Monitoring of Splitting Failure in Reinforced Concrete," *Journal of Nondestructive Evaluation*, vol. 32, no. 4, pp. 372–383, Dec. 2013, https://doi.org/10.1007/s10921-013-0191-y.

[43] V. Revilla-Cuesta, M. Skaf, F. Faleschini, J. M. Manso, and V. Ortega-López, "Self-compacting concrete manufactured with recycled concrete aggregate: An overview," *Journal of Cleaner Production*, vol. 262, Jul. 2020, Art. no. 121362, https://doi.org/10.1016/j.jclepro.2020.121362.

[44] R. Bani Ardalan, A. Joshaghani, and R. D. Hooton, "Workability retention and compressive strength of self-compacting concrete incorporating pumice powder and silica fume," *Construction and Building Materials*, vol. 134, pp. 116–122, Mar. 2017, https://doi.org/10.1016/j.conbuildmat.2016.12.090.

[45] X. Shi, P. Park, Y. Rew, K. Huang, and C. Sim, "Constitutive behaviors of steel fiber reinforced concrete under uniaxial compression and tension," *Construction and Building Materials*, vol. 233, Feb. 2020, Art. no. 117316, https://doi.org/10.1016/j.conbuildmat.2019.117316.